

FREQUENCY-TEMPERATURE DEPENDENCE OF POLYMER
COMPLEX MODULUS PROPERTIES

by

Tom Lewis and Ahid D. Nashif
Anatrol Corporation, Cincinnati, Ohio 45241

and

David I.G. Jones
Materials Laboratory (AFWAL/MLLN)
Wright-Patterson AFB, Ohio 45433

ABSTRACT

Advances in the frequency-temperature analysis of complex modulus properties of polymeric materials are described. Means are identified for minimizing the errors in data analysis for determination of parameters in an Arrhenius shift-factor relationship. The approach is illustrated for data obtained by several test methods, for a commercial polymeric viscoelastic adhesive, over wide frequency and temperature ranges.

INTRODUCTION

It has long been recognized that the complex modulus behavior of polymeric viscoelastic materials depends on temperature and frequency through a combined variable which is the product of the frequency and a function of the temperature. The form of this function depends on the particular material being investigated, and is determined in principle by examining plots of $\log(\text{modulus})$ and $\log(\text{loss factor})$ versus $\log(\text{frequency})$, and determining the necessary shift along the $\log(\text{frequency})$ axis required to collapse all the data points on to a unique pair of master curves. This process is considered to be applicable only to thermo-rheologically simple materials, but practical experience indicates very broad applicability of the approach. The current state of the art is such that most experimental data for specific materials is subject to systematic and random errors, often of significant magnitude, and the problems of determining reliable estimates of the shift factors are compounded by these errors and by the limited frequency and temperature ranges over which data is obtained. It is not usually possible to completely overcome these problems for any given data set, except by additional more carefully conducted testing, but some measure of data qualification can be achieved relatively simply.

The first step is to create a plot of $\log(\text{loss factor})$ versus $\log(\text{modulus})$, using every experimental point available at all frequencies and temperatures. This process, which is becoming quite widely applied, eliminates frequency and temperature as independent variables, and the resulting graph should have all the points clustered along a unique, smooth curve. Points deviating too far from the majority may be eliminated as being in error, if for unknown reasons. Following this, detailed examination of the plots of $\log(\text{modulus})$ and $\log(\text{loss factor})$ versus frequency, for each temperature, will also allow one to identify points which deviate too far from the main body of data. In this way, one may be sure of having more consistent data, if not more accurate data.

The next step is to postulate a definite relationship between the shift factor required to merge all data into a set of unique master curves and the temperature. This relationship should have one or more selectable parameters. The simplest relationship, usually referred to as an Arrhenius relationship, is a linear plot of $\log(\text{shift factor})$ versus inverse absolute temperature. The selectable parameters, the activation energy, and the reference temperature are varied until the scatter in the master curves is a minimum. The process can often be simplified even further by analyzing not the modulus and loss factor versus frequency, but rather a modulus ratio incorporating the estimated minimum and maximum modulus values and the loss factor.

ANALYSIS

The starting point for frequency-temperature analysis of complex modulus properties is the assumed relationships:

$$E_r = (T_0/T) E(f_r) \quad (1)$$

$$\eta_r = \eta(f_r) \quad (2)$$

$$f_r = f\alpha(T) \quad (3)$$

$$\text{with } \log\alpha(T) = T_A/T - T_A/T_0 \quad (4)$$

for an Arrhenius type shift factor relationship. The "activation temperature" T_A is equal to $Q/2.303R$, where Q is the activation energy and R is the Universal Gas Constant. Q is a function of temperature, in general, but there is considerable evidence that it is constant over fairly wide temperature ranges when only one major mechanism of energy dissipation is dominant. T_0 is the reference temperature, which may be chosen arbitrarily, although a temperature within the transition region is usually selected. Equations (3) and (4) define a temperature-compensated frequency $f_r = f \exp(Q/RT)$, on which the modulus (E or G) and the loss factor (η) depend. The ratio T_0/T (or more precisely $\rho_0 T_0/\rho T$) allows for bulk expansion of the sample as a function of absolute temperature, and is often approximated by 1.0 for simplicity and convenience. Further simplification of the analysis is achieved by postulating a simple relationship between E_r and f_r [1] of the form:

$$E_r(f_r) = E_{r\infty} - (E_{r\infty} - E_{r0}) \frac{1}{1 + \beta(f_r)^n} \quad (5)$$

which may be re-stated in the form:

$$E_e = \frac{E_r(f_r) - E_{r0}}{E_{r\infty} - E_r(f_r)} = \beta(f_r)^n \quad (6)$$

$$\log(E_e) = n \log(f_r) + \log(\beta) \quad (7)$$

where E_{r0} is the asymptotic value of E_r at zero frequency (f_r) and $E_{r\infty}$ is the asymptotic value of E_r at infinite value of f_r . Equation (7) implies a linear relationship between $\log(E_e)$ and $\log(f_r)$, and forms the basis for a simple linear regression analysis of the test data.

$$\text{Furthermore } n_r = \frac{K2(f_r)^{(p-1)}}{(1+K3(f_r)^p)^m} \quad (8)$$

A prior investigation [2] has shown that an Arrhenius model fully describes the frequency-temperature behavior of a specific polymer, and that other equations such as the WLF equation represent modest deviations from the Arrhenius model which are often not supported by the experimental data, especially in view of the scatter usually encountered. This is the basis for the foregoing, very simple analysis. The further introduction of a modulus ratio E_e , which is assumed to be a simple function of the reduced frequency f_r allows one to utilize simple statistical methods for determining the optimum value of the activation temperature T_A . Both of these simplifications not only simplify computer-based analysis of the data, but represent also a simple physical-mathematical model which may be verified for each material on the basis of how well it fits the experimental data. So far, no data has been encountered which fails to fit this type of model. The illustration which follows, demonstrating the application of the approach to a viscoelastic adhesive, is typical.

ILLUSTRATION

The approach just described will be applied to a data set obtained for a commercial viscoelastic adhesive, 3M-966 [3], by several test techniques. Complex modulus properties were measured by the ASTM standard vibrating beam test and by relaxation and impedance methods. The test techniques have been described adequately elsewhere [1,4,5]. The measured complex modulus data, for shear deformations, is summarized in Table 1. Figure 1 shows a plot of frequency versus temperature, which identifies the conditions pertaining to each test point and test method. It is seen that many points were obtained between -50°F and 250°F , and between 100 Hz and 10,000 Hz, a few between 0°F and 100°F and between $1\text{E-}4$ Hz and 0.1 Hz, but that a gap appears between 0.1 Hz and 50 Hz for all temperatures. No test technique was fully satisfactory in this region. Efforts to develop improved techniques for data acquisition in the gap area are under way, but even without such data, the data readily collapses by the reduced-variables method outlined earlier. Figure 2 shows the standard plot of $\log(\text{loss factor})$ versus $\log(\text{modulus})$. Some points which deviated significantly from the main body of data were culled from the data set.

The next step in the data reduction process was to apply an Arrhenius type of shift process, in accordance with equation (4), and vary the activation temperature T_A until scatter in the plots of $\log(\text{modulus})$ and $\log(\text{loss factor})$ versus $\log(\text{reduced frequency})$ is minimized. This process is illustrated in Figures 3 through 11 for values of T_A equal to 5000, 7000, 8000, 8900, 10000, 11000, 12000, 13000, and 15000 $^{\circ}$ R. It is seen that the low frequency data, in particular, serves to indicate deviation from full collapse. The figures show the progressive reduction of scatter to an optimum near $T_A = 8900^{\circ}$ R, with greater errors for lower and higher values of T_A . The scatter may be measured in several ways, including visual judgement, plotting of the progression of the gap between selected pairs of points, or through more elaborate statistical analysis of a larger number of selected points.

Following the first identification of an optimum value of T_A , the plots may also indicate the possibility that an Arrhenius model may not be completely satisfactory. As Figure 6 shows, however, for $T_A = 8900$ very few points clearly indicate deviations from the "linear" shift factor relationship implied in equation (4). In fact, no material data has yet been identified for which the deviation from this type of "linearity" is sufficiently large to be visible over the general level of scatter in the data.

Further iteration of the identification process may now be exercised by examining the plots of $\log(G_p)$ versus $\log(\text{reduced frequency})$, as defined by equations (5) to (7). These plots are summarized in Figures 12 to 20, for the same values of T_A and for $G_0 = 8 \text{ Lb/in}^2$ and $G_{\infty} = 1.5e5 \text{ Lb/in}^2$. Again, the scatter reduces as T_A approaches the optimum value of about 8900 $^{\circ}$ R. The iterative process now involves careful analysis of the effects of varying G_0 and G_{∞} as well as T_A until the plot is as linear as possible and the scatter a minimum. Simple statistical analysis may be applied.

Finally, a nomogram may be created in the usual way [1], as shown in Figure 21. This completes the data analysis for this specific material. Similar data analyses have been conducted for 3M-966 in tension-compression and for many other materials. The "linear" Arrhenius model of the shift factor behavior with respect to temperature seems to apply in every case, and no deviations have been observed within the limits of scatter. The significance of this is still not fully understood.

CONCLUSIONS

It has been shown that a "linear" Arrhenius model for the dependence of frequency-temperature shift factors on temperature is effective for producing low scatter "master" plots of complex modulus properties versus a reduced frequency depending on frequency and temperature. The approach has been illustrated for a specific material. Other data supports the same conclusion. The simplicity of the Arrhenius relationship, along with the initial assumption of a simple relationship between modulus and

reduced frequency further allows simple linear regression analysis to be applied to the search for the optimum value of the activation temperature, which is a direct measure of the activation energy.

REFERENCES

1. A.D. Nashif, D.I.G. Jones and J.P. Henderson, *Vibration Damping*, Wiley Interscience, 1985.
2. D.I.G. Jones, A.D. Nashif and D.K. Rao, "Investigation of Shift Factors in Material Damping," ASME Paper 87-WA/AERO-7, Presented at ASME Winter Annual Meeting, Boston, MA, Dec. 1987.
3. 3M-966 Viscoelastic Damping Adhesive, 3M Company, St. Paul, MN.
4. ASTM Standard E756-80, "Standard Method for Measuring Vibration-Damping Properties of Materials," 1980.
5. M.L. Parin, A.D. Nashif and T.M. Lewis, "Relsat Damping Material Data," AFWAL-TR-86-3059, Vol. 1, pp AD-1 to AD-80, 1986.

Table 1: Complex Modulus Data - 3M Y-966

10" Sandwich Beam

<u>Temperature</u>	<u>Frequency</u>	<u>Modulus</u>	<u>Loss Factor</u>
94.33	134.18	75.83	1.313057
94.33	366.06	119.91	1.471784
94.33	708.23	155.60	1.352790
94.33	1167.19	260.90	1.297942
94.33	1739.49	311.56	1.251339
114.00	131.59	52.21	0.954046
114.00	359.55	61.30	1.259684
114.00	702.18	106.12	0.969221
114.00	1152.72	122.02	1.299971
114.00	1724.19	171.99	1.141671
134.00	129.29	30.39	0.883965
134.00	357.32	44.00	0.960007
134.00	696.54	59.73	0.913520
134.00	1147.93	87.67	0.922173
134.00	1715.25	100.85	1.008548
153.63	128.35	22.41	0.706620
153.83	355.28	28.36	0.868475
153.83	1709.91	67.98	0.866073
174.00	127.65	16.81	0.584690
174.00	354.17	21.96	0.693342
233.17	126.20	6.31	0.226837
253.00	126.10	6.63	0.169085
253.00	350.97	7.84	0.220534
55.80	169.90	460.54	1.429654
55.80	782.36	930.38	0.857959
55.80	1898.74	2060.02	1.039232
65.25	154.80	309.50	0.999700
65.25	761.69	663.70	1.491555
65.25	1833.27	1320.26	0.958539
74.40	154.28	309.31	0.892138
74.40	391.65	378.94	1.161334
74.40	1204.48	658.90	0.952200
74.40	1789.95	839.49	1.047756
85.00	139.81	132.31	1.295457
85.00	377.36	234.06	1.101109
85.00	718.61	255.44	1.129037
85.00	1176.33	350.73	1.360883
65.00	1760.87	532.12	1.123667
70.40	393.59	387.19	1.421225
70.40	753.82	615.02	0.983556
70.40	1873.74	1836.24	0.628351
43.00	201.33	1100.83	1.013737
43.00	956.47	3598.22	0.522952
29.67	237.22	2839.00	0.702139
29.67	592.87	4460.24	0.660257
29.67	1092.90	7119.03	0.381514
20.50	256.79	5230.67	0.594997
20.50	670.60	8735.28	0.630281
11.00	268.39	9120.56	0.390761
11.00	698.17	12861.83	0.390824

Table 1: Complex Modulus Data - 3M Y-966 (Con't.)

10" Sandwich Beam (Con't.)

<u>Temperature</u>	<u>Frequency</u>	<u>Modulus</u>	<u>Loss Factor</u>
2.25	276.60	14505.64	0.312686
2.25	733.90	20638.89	0.277731
2.25	1334.38	22239.30	0.244773
2.25	1977.63	20316.67	0.220431
-7.50	281.90	21819.36	0.226373
-7.50	755.38	29109.55	0.205839
-7.50	1406.68	33452.94	0.233467
-7.50	2143.24	31346.35	0.248907
-16.50	285.59	31386.20	0.175795
-16.50	772.46	40569.11	0.142938
-16.50	2269.37	46608.91	0.102699
-33.00	787.46	57987.82	0.073777
-33.00	1484.05	59747.66	0.111454
-33.00	2360.83	63172.90	0.058559
-49.00	795.07	71529.93	0.048820
-49.00	1499.56	66480.48	0.047705
-49.00	2404.18	73744.40	0.039597

5" Sandwich Beam

<u>Temperature</u>	<u>Frequency</u>	<u>Modulus</u>	<u>Loss Factor</u>
-47.00	5000.00	71601.62	0.043944
-25.00	1122.85	43884.45	0.078826
-25.00	2760.72	52564.42	0.081239
-25.00	4838.90	61488.95	0.082077
-8.00	1059.69	28380.08	0.176317
-8.00	2551.63	34920.95	0.183963
-8.00	4434.21	41254.14	0.188414
9.00	952.00	14931.14	0.344016
26.00	821.54	7202.87	0.560541
26.00	1953.31	9970.31	0.360439
26.00	3450.49	11749.96	0.485872
46.67	666.43	2631.76	0.858444
46.67	1606.08	2736.74	0.935332
46.67	3036.27	4132.80	0.777935
58.00	1519.18	1428.80	1.009958
58.00	2914.09	2243.93	0.892514
72.00	538.78	454.95	1.142293
72.00	1469.46	729.50	0.926019
72.00	2840.06	1164.90	0.829148
92.50	520.21	198.03	1.064238
92.50	1439.97	325.81	0.965631

Table 1: Complex Modulus Data - 3M Y-966 (Con't.)

Shear Relaxation

<u>Temperature</u>	<u>Frequency</u>	<u>Modulus</u>	<u>Loss Factor</u>
0.00	1.380E-004	10.29	0.307000
0.00	2.800E-004	11.58	0.394000
0.00	5.600E-004	13.43	0.484000
0.00	1.110E-003	16.02	0.585000
0.00	2.220E-003	19.53	0.699700
0.00	4.450E-003	24.61	0.816000
0.00	8.900E-003	31.56	0.971000
0.00	1.780E-002	42.81	1.094000
0.00	3.560E-002	76.90	1.122300
26.00	1.400E-004	6.79	0.117250
26.00	2.800E-004	7.12	0.153000
26.00	5.600E-004	7.56	0.202000
26.00	1.110E-003	8.13	0.265000
26.00	2.220E-003	8.98	0.358000
26.00	4.450E-003	10.24	0.447100
26.00	8.890E-003	11.68	0.565000
26.00	1.778E-002	13.82	0.756000

SDOF Resonance

<u>Temperature</u>	<u>Frequency</u>	<u>Modulus</u>	<u>Loss Factor</u>
93.00	109.40	42.77	0.968000
125.00	72.50	18.90	0.720000
150.00	69.46	17.36	0.670000
175.00	56.27	11.40	0.550000
25.00	2041.70	15006.70	0.330000
0.00	3115.60	34945.00	0.200000
50.00	725.79	1896.40	0.580000
80.00	182.08	119.40	1.000000

Table 1: Complex Modulus Data - 3M Y-966 (Con't.)

SDOF Shear Impedance

<u>Temperature</u>	<u>Frequency</u>	<u>Modulus</u>	<u>Loss Factor</u>
150.00	71.88	17.20	1.039500
150.00	90.63	20.60	0.974600
150.00	109.38	22.20	0.955300
150.00	131.25	25.20	0.914900
150.00	150.00	28.30	0.894800
150.00	171.88	32.60	0.840000
150.00	190.63	33.30	0.816500
175.00	90.63	14.30	0.725600
175.00	109.38	18.80	0.569200
175.00	131.25	21.80	0.640700
25.00	1609.38	14347.80	0.486800
25.00	1903.13	14731.60	0.471200
25.00	2003.13	14815.40	0.445800
25.00	2103.13	15032.70	0.444000
25.00	2203.13	15265.30	0.424100
25.00	2303.13	15635.00	0.409500
25.00	2403.13	15829.00	0.399200
25.00	2503.13	16241.00	0.382900
25.00	2603.13	16407.10	0.380000
25.00	2703.13	16838.20	0.357500
25.00	2803.13	17046.30	0.349800
25.00	2903.13	17406.00	0.350000
25.00	2996.88	17867.70	0.329200
0.00	2718.75	34259.40	0.236600
0.00	2806.25	34353.40	0.229100
0.00	2900.00	34340.20	0.220600
0.00	3000.00	34586.60	0.219300
0.00	3100.00	34632.60	0.213800
0.00	3200.00	34810.20	0.208900
0.00	3300.00	34982.20	0.204200
0.00	3400.00	35294.00	0.198500
0.00	3500.00	35641.30	0.194200
0.00	3600.00	35890.00	0.194500
0.00	3700.00	36038.70	0.189000
0.00	3800.00	36414.30	0.178000
0.00	3900.00	36806.90	0.178400
0.00	4000.00	37158.30	0.168500
50.00	706.25	1761.00	1.155600
50.00	900.00	2250.60	0.940100
50.00	1100.00	2556.50	0.831200
50.00	1300.00	2948.70	0.764500
50.00	1500.00	3333.30	0.696100
50.00	1700.00	3808.20	0.616900
50.00	1900.00	4221.40	0.574700
50.00	2000.00	4447.10	0.505900

Table 1: Complex Modulus Data - 3M Y-966 (Con't.)

SDOF Shear Impedance (Con't.)

<u>Temperature</u>	<u>Frequency</u>	<u>Modulus</u>	<u>Loss Factor</u>
80.00	200.00	127.30	1.630000
80.00	300.00	195.00	1.261100
60.00	400.00	254.20	1.102700
80.00	500.00	312.70	0.998900
60.00	600.00	390.60	0.893200
60.00	700.00	469.10	0.815600
93.00	150.00	60.00	1.455000
93.00	162.50	63.70	1.412400
93.00	175.00	68.20	1.371400
93.00	187.50	71.70	1.338700
93.00	200.00	77.60	1.278700
125.00	90.63	21.60	1.074300
125.00	112.50	24.70	1.041100
125.00	131.25	26.50	0.944200
125.00	150.00	32.20	0.868800
125.00	171.88	35.80	0.848900
125.00	190.63	40.40	0.823900
125.00	200.00	42.20	0.794500

Shear Creep

<u>Temperature</u>	<u>Frequency</u>	<u>Modulus</u>	<u>Loss Factor</u>
62.00	1.995E-003	6.05	0.125120
62.00	3.990E-003	6.41	0.142020
62.00	7.980E-003	6.80	0.149730
62.00	1.596E-002	7.30	0.177180
62.00	3.192E-002	7.73	0.206000
62.00	6.384E-002	8.34	0.255640
62.00	1.277E-001	9.76	0.295020

FAC-12

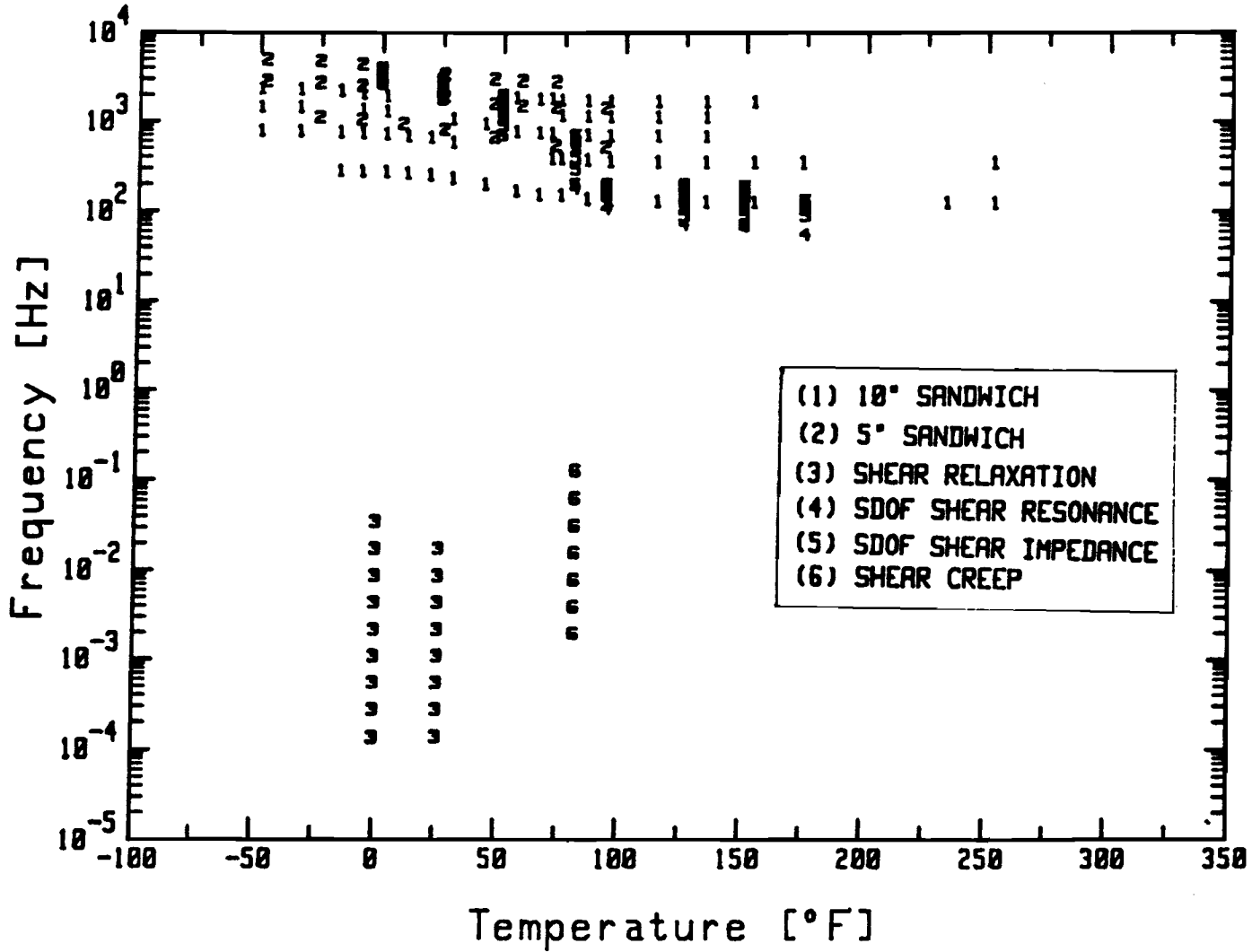


Figure 1: All Data Points Plotted Versus Temperature and Frequency, Illustrating the Areas Covered/Not Covered by the Test Techniques Used

FAG-13

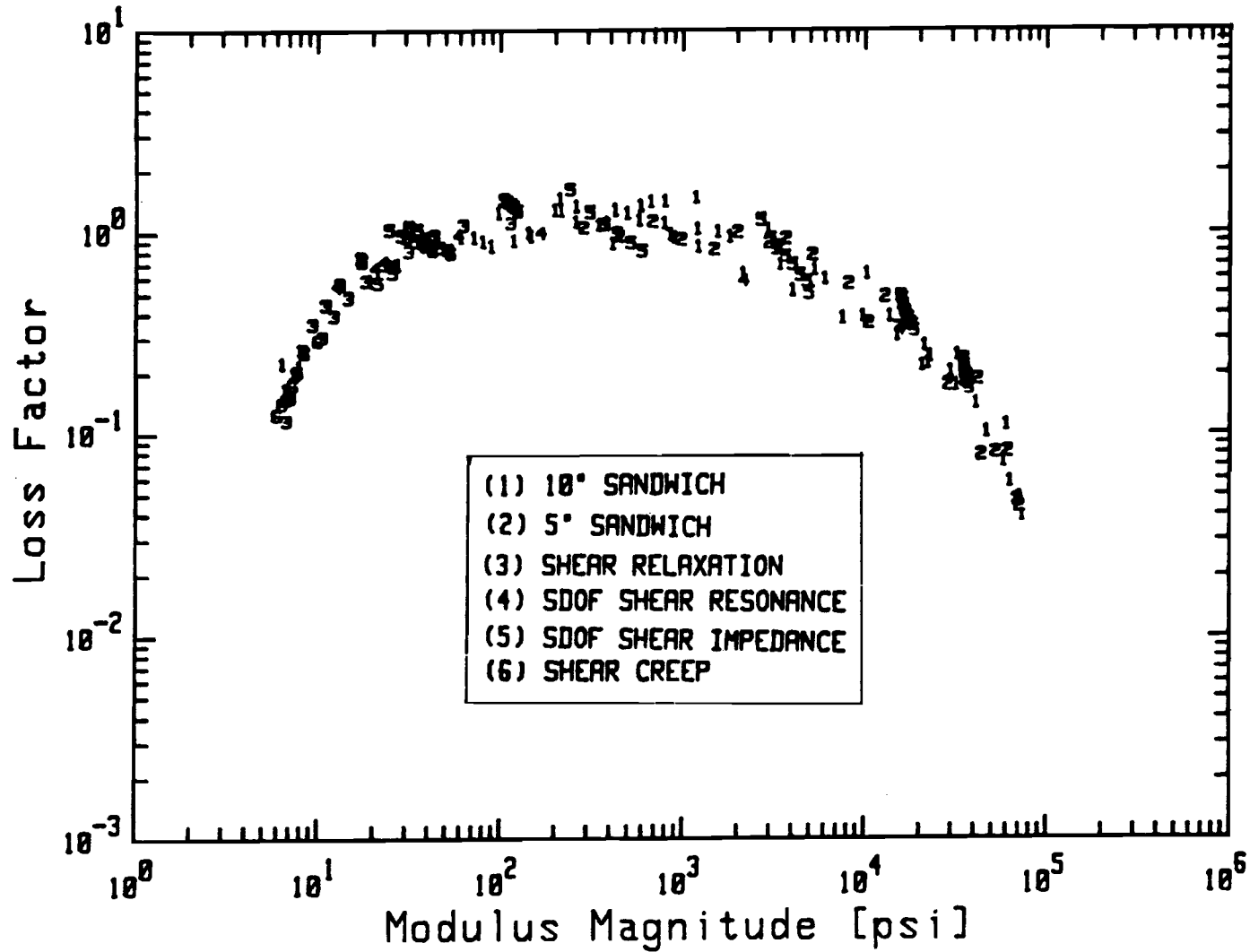


Figure 2: Plot of Loss Factor Versus Modulus, Showing Measure of Uniqueness of Relationship Between the Real and Imaginary Parts of the Complex Modulus

FAC-14

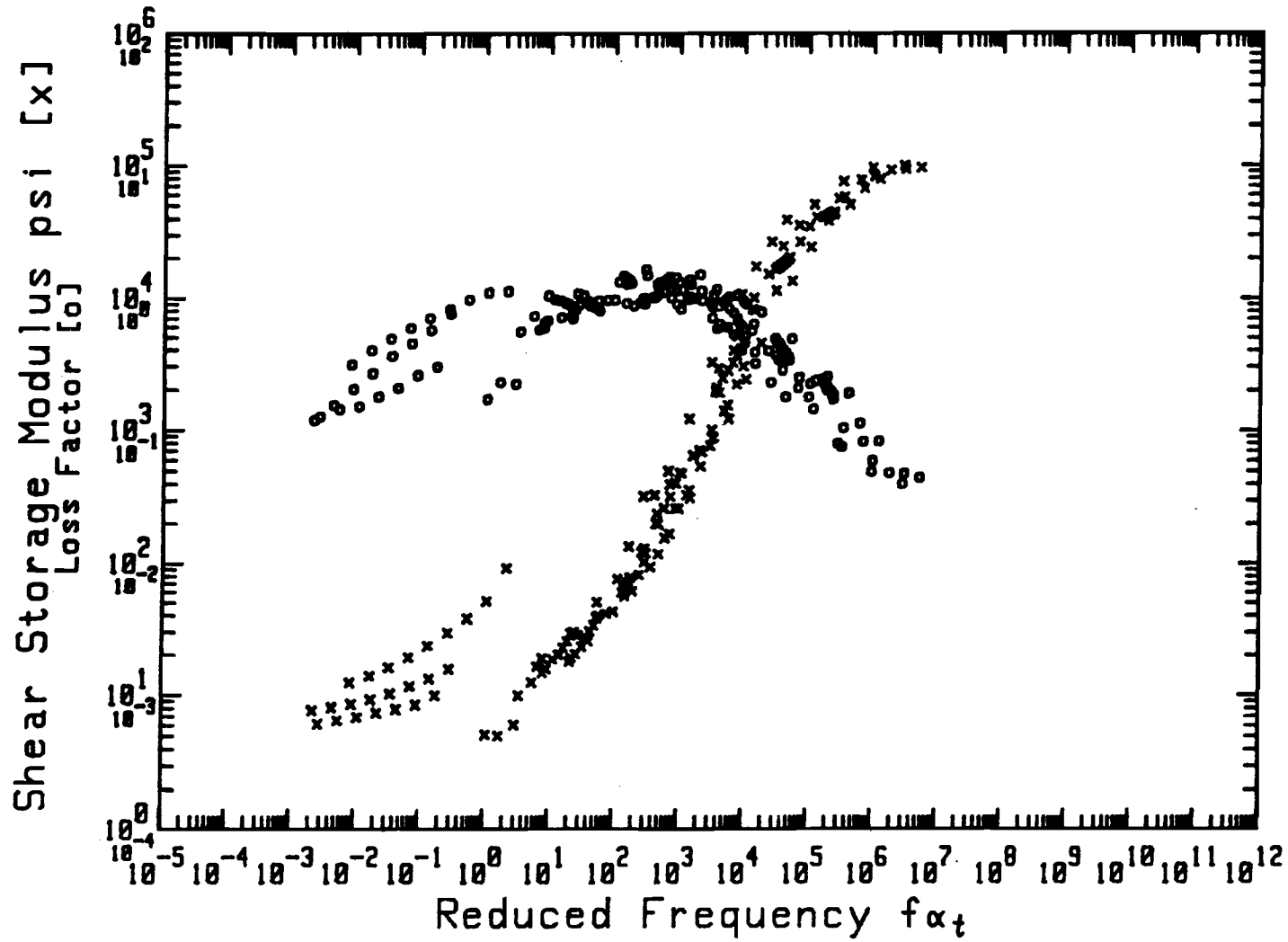


Figure 3: Plot of Shear Modulus and Loss Factor Versus Reduced Frequency ($T_A = 5000^\circ R$)

FAC-15

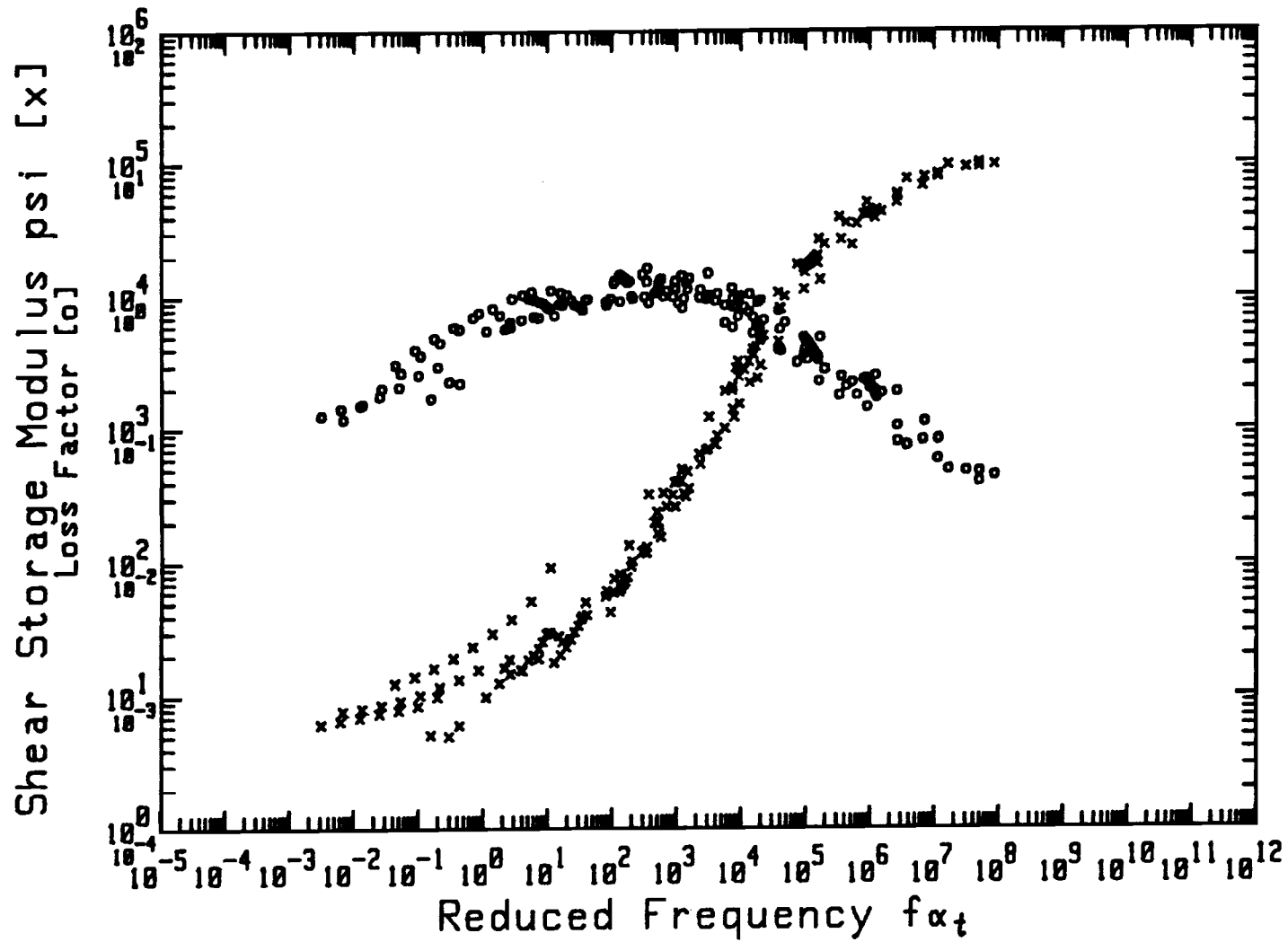


Figure 4: Plot of Shear Modulus and Loss Factor Versus Reduced Frequency ($T_A = 7000^\circ R$)

FAC-16

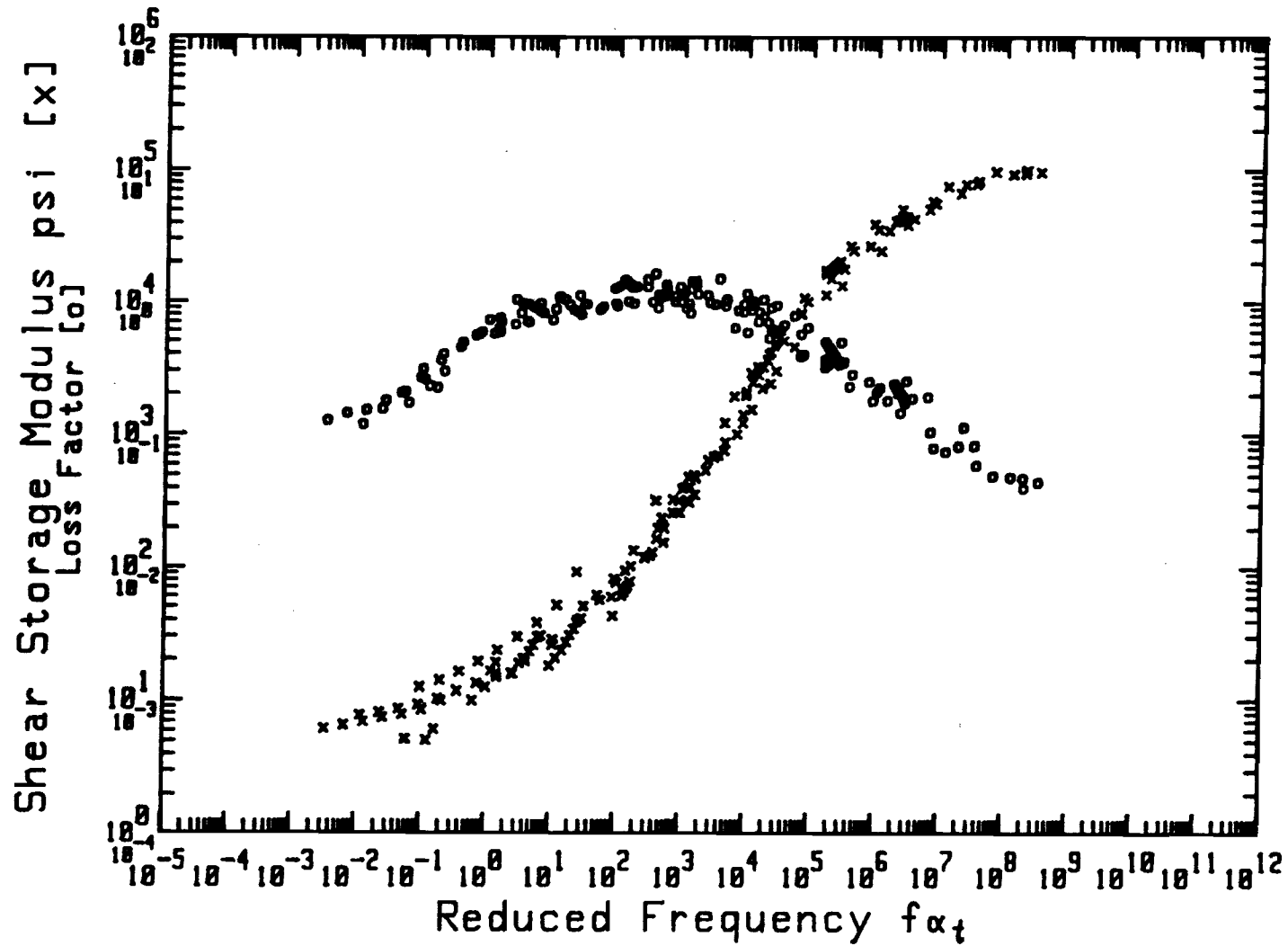


Figure 5: Plot of Shear Modulus and Loss Factor Versus Reduced Frequency ($T_A = 8000^\circ R$)

contrails.uit.edu

FAC-17

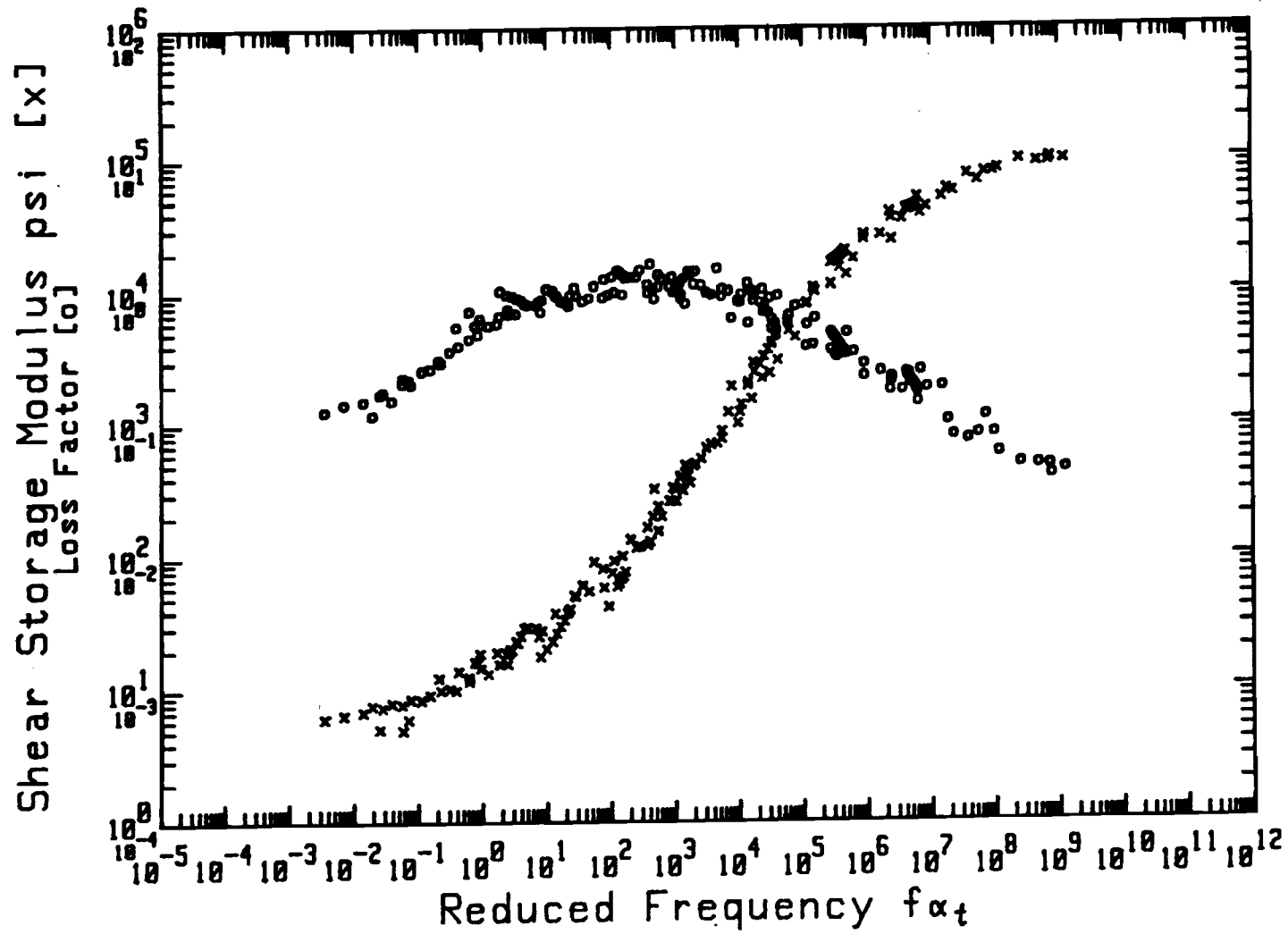


Figure 6: Plot of Shear Modulus and Loss Factor Versus Reduced Frequency
($T_A = 8900^\circ\text{R}$)

FAC-18



Figure 7: Plot of Shear Modulus and Loss Factor Versus Reduced Frequency ($T_A = 10000^\circ R$)

FAC-19

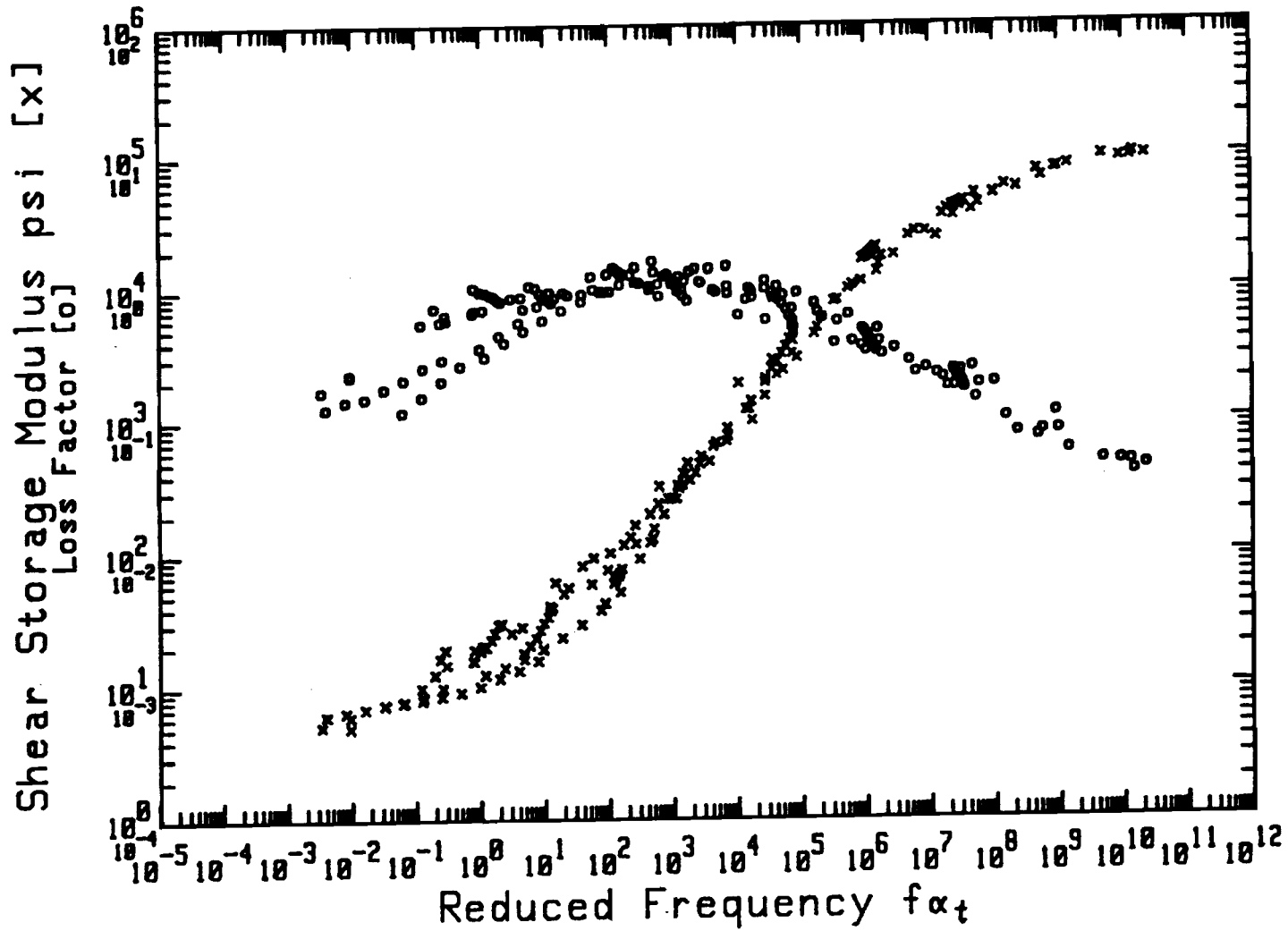


Figure 8: Plot of Shear Modulus and Loss Factor Versus Reduced Frequency
 ($T_A = 11000^\circ R$)

contrails.uit.edu

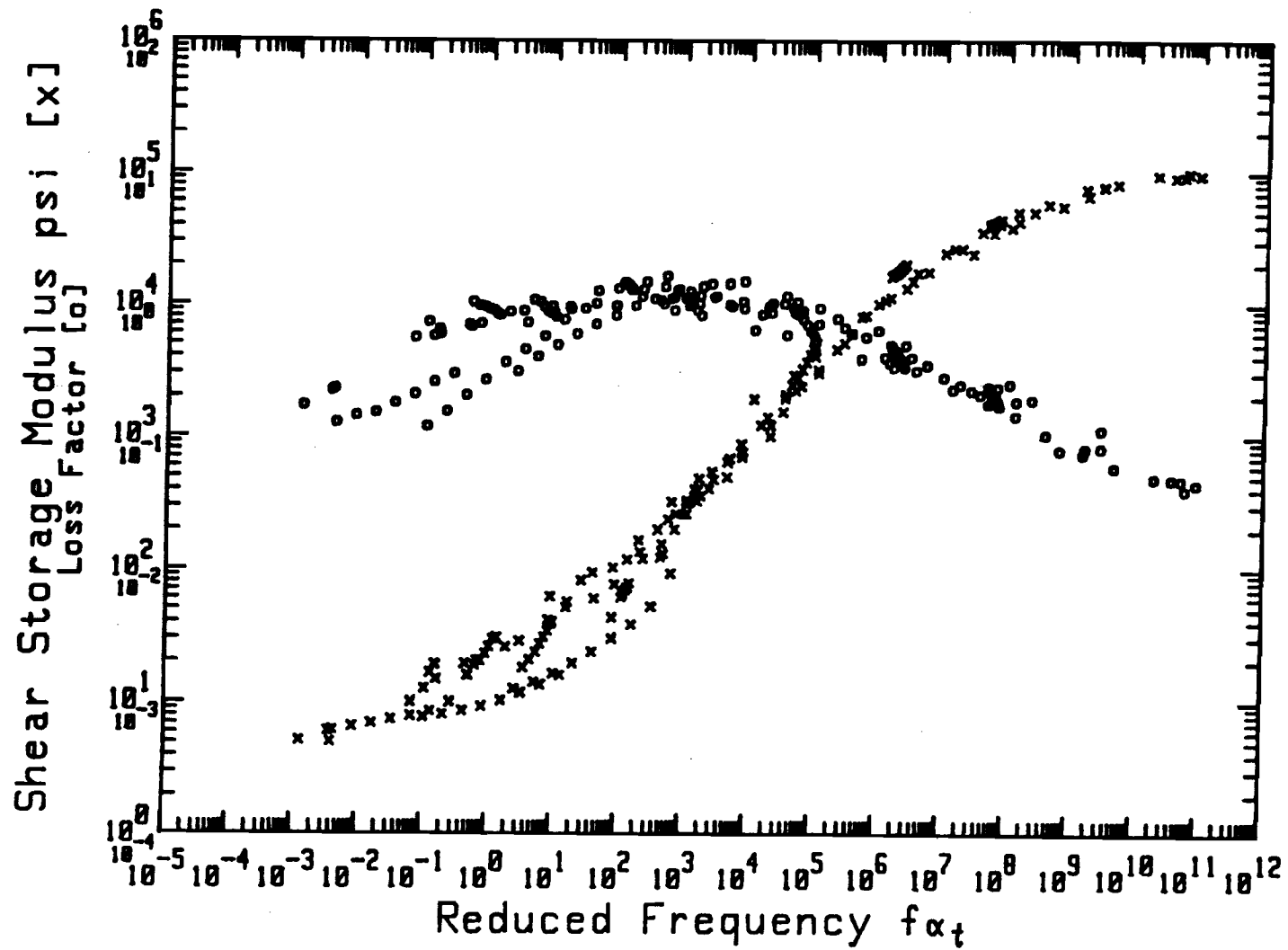


Figure 9: Plot of Shear Modulus and Loss Factor Versus Reduced Frequency
($T_A = 12000^\circ R$)

FAC-21

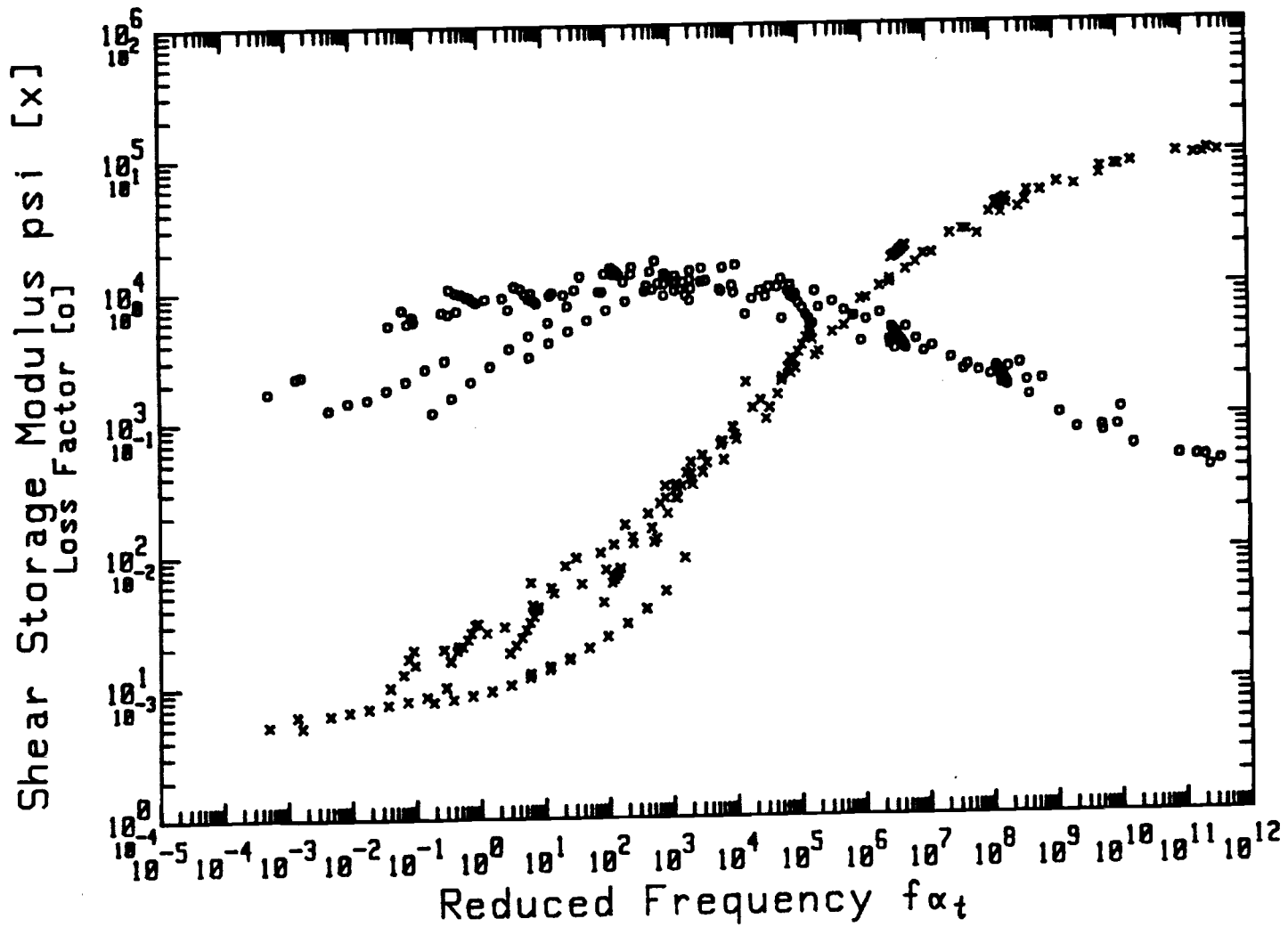


Figure 10: Plot of Shear Modulus and Loss Factor Versus Reduced Frequency
 (T_A = 13000°R)

FAC-22

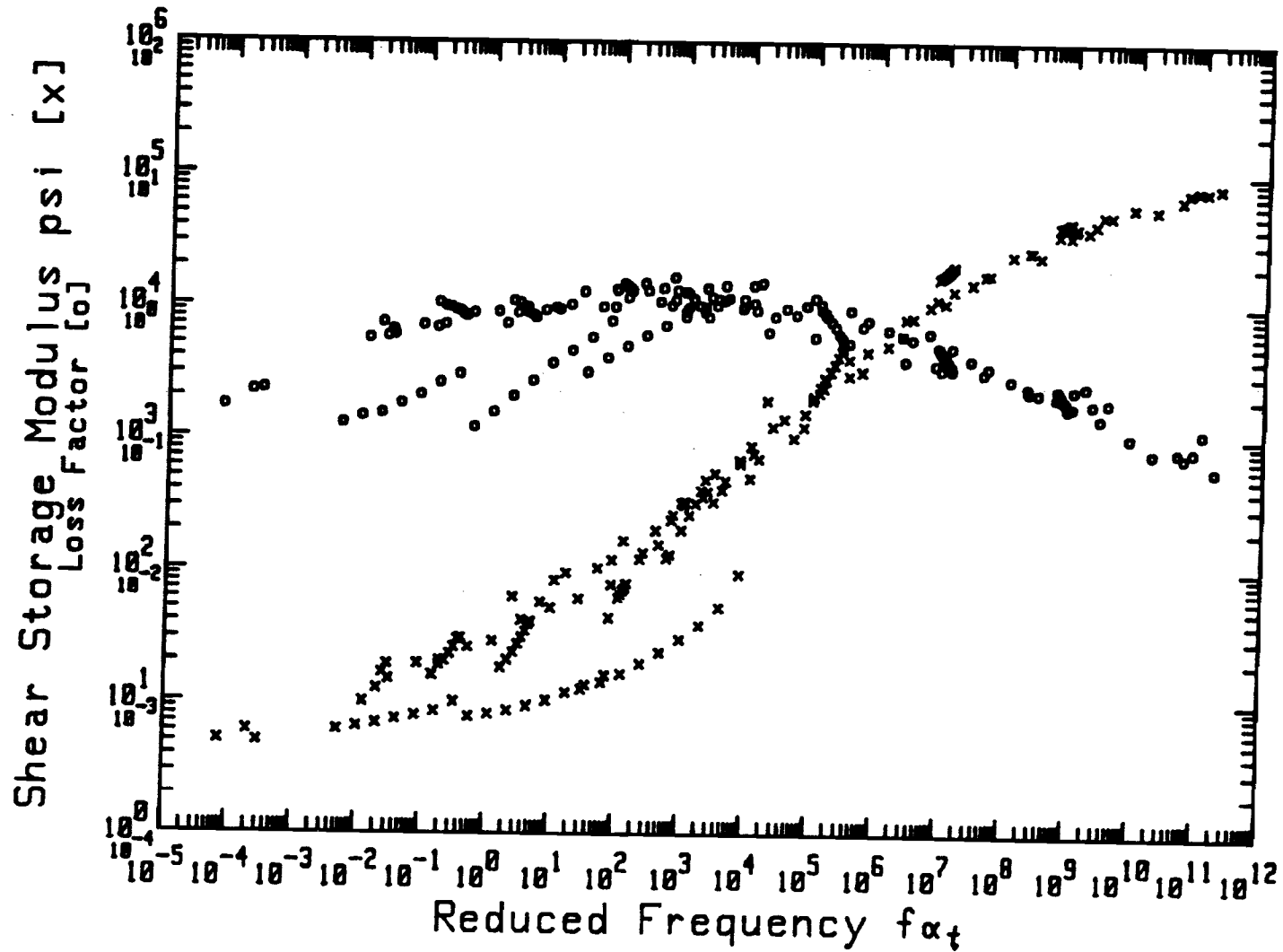


Figure 11: Plot of Shear Modulus and Loss Factor Versus Reduced Frequency ($T_A = 15000^\circ R$)

FAC-23

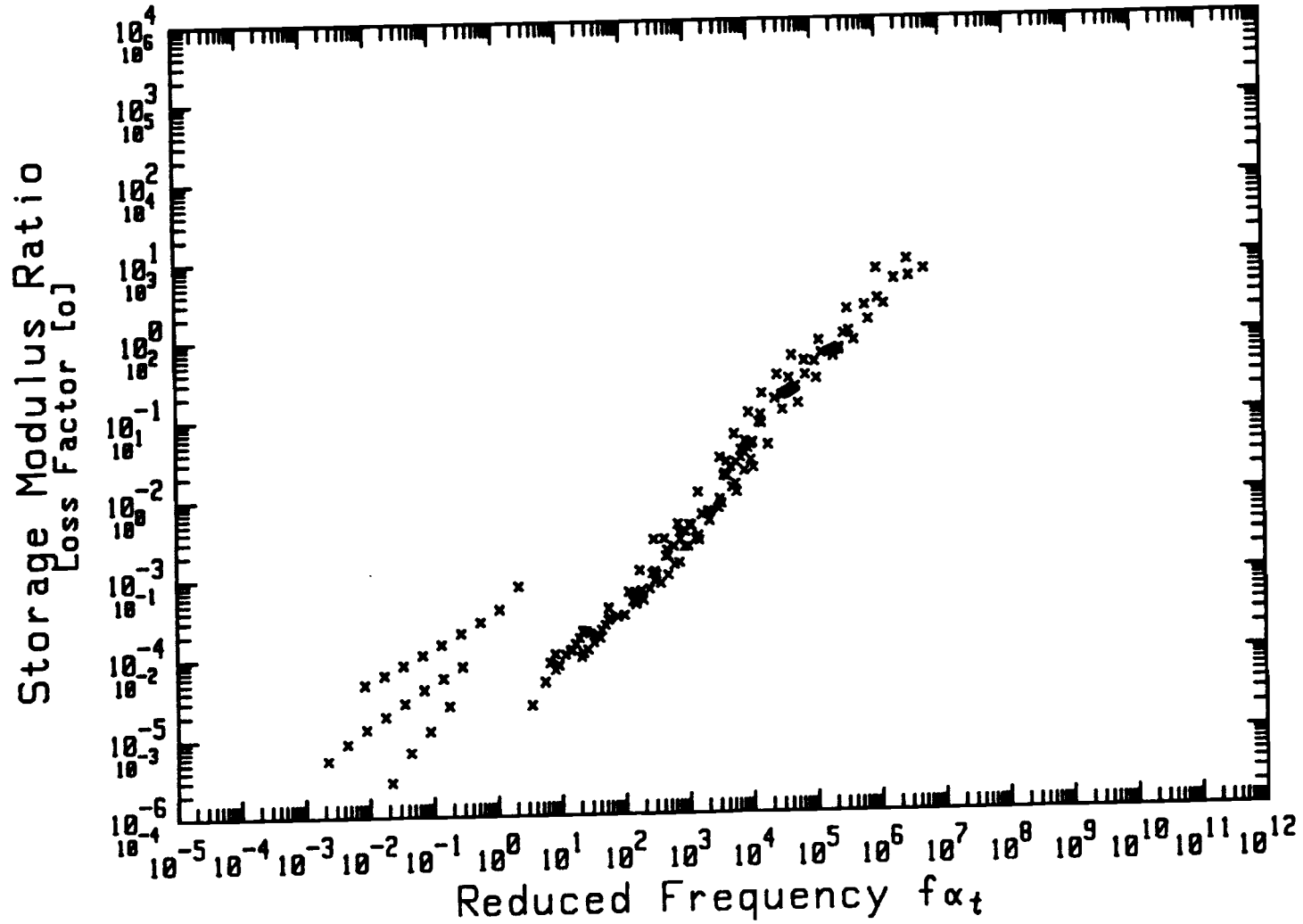


Figure 12: Plot of Modulus Ratio (G_e) Versus Reduced Frequency ($T_A = 5000^\circ R$)

FAC-24

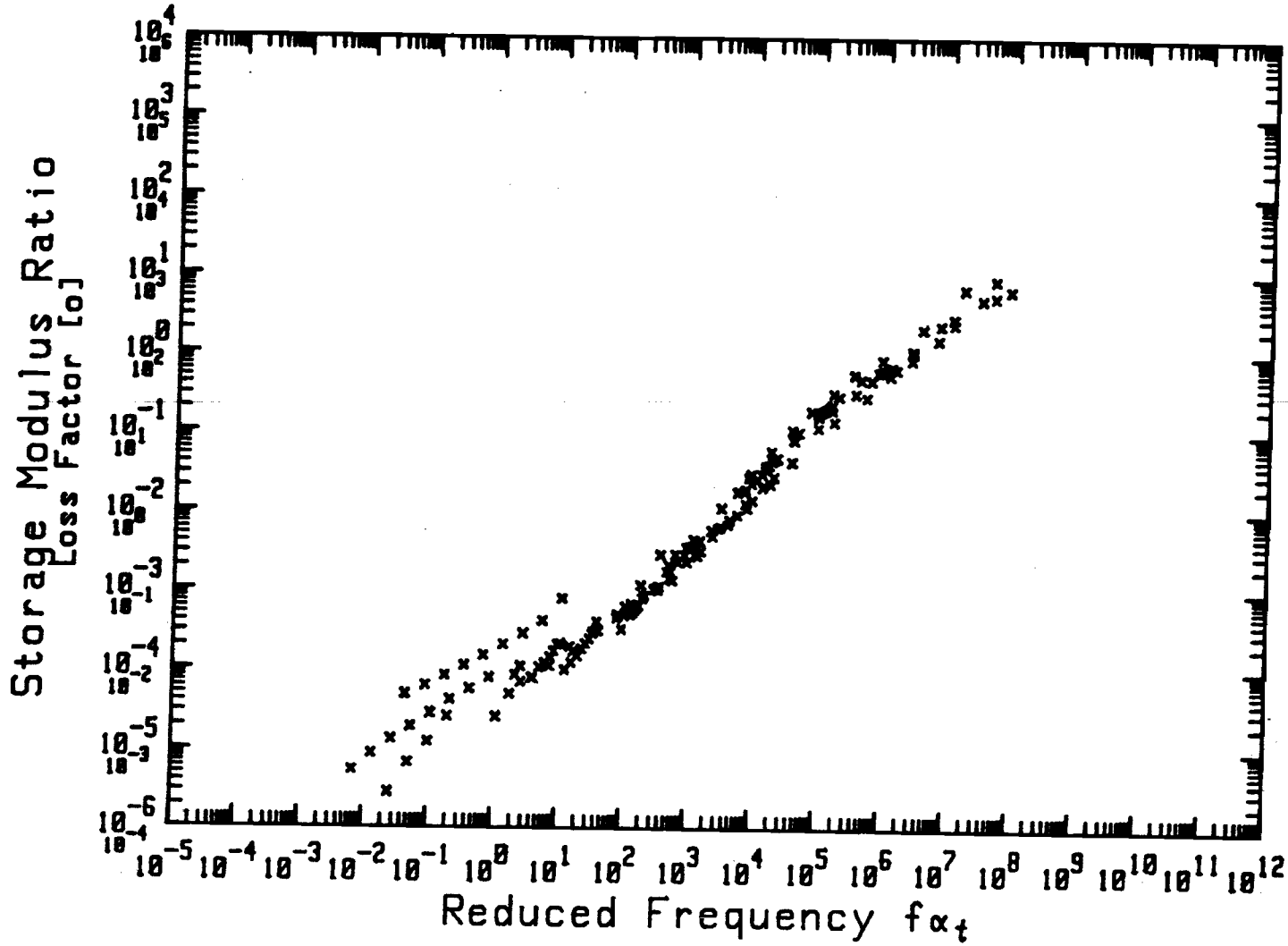


Figure 13: Plot of Modulus Ratio (G_e) Versus Reduced Frequency ($T_A = 7000^\circ R$)

FAC-25

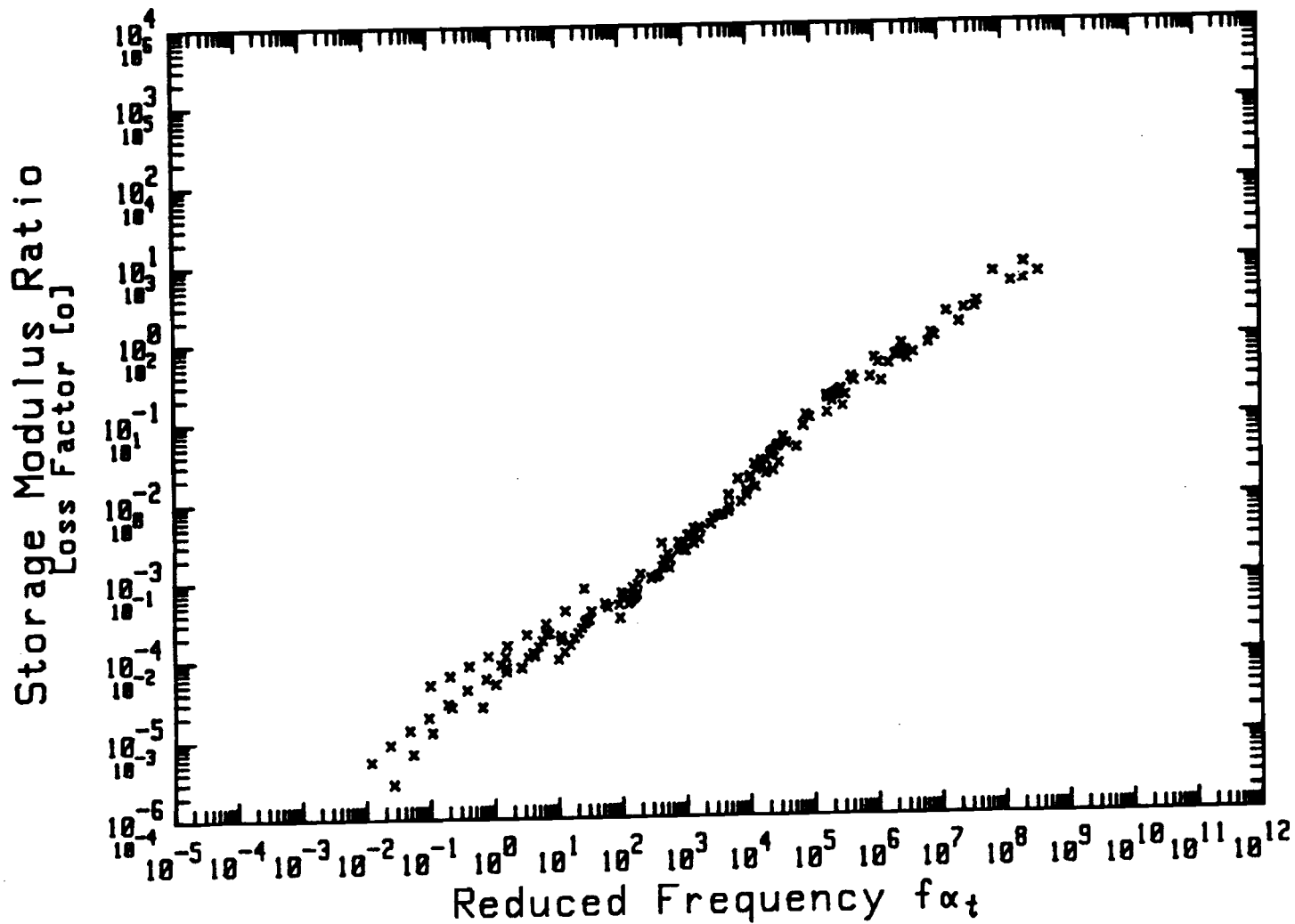


Figure 14: Plot of Modulus Ratio (G_e) Versus Reduced Frequency ($T_A = 8000^\circ R$)

FAC-26

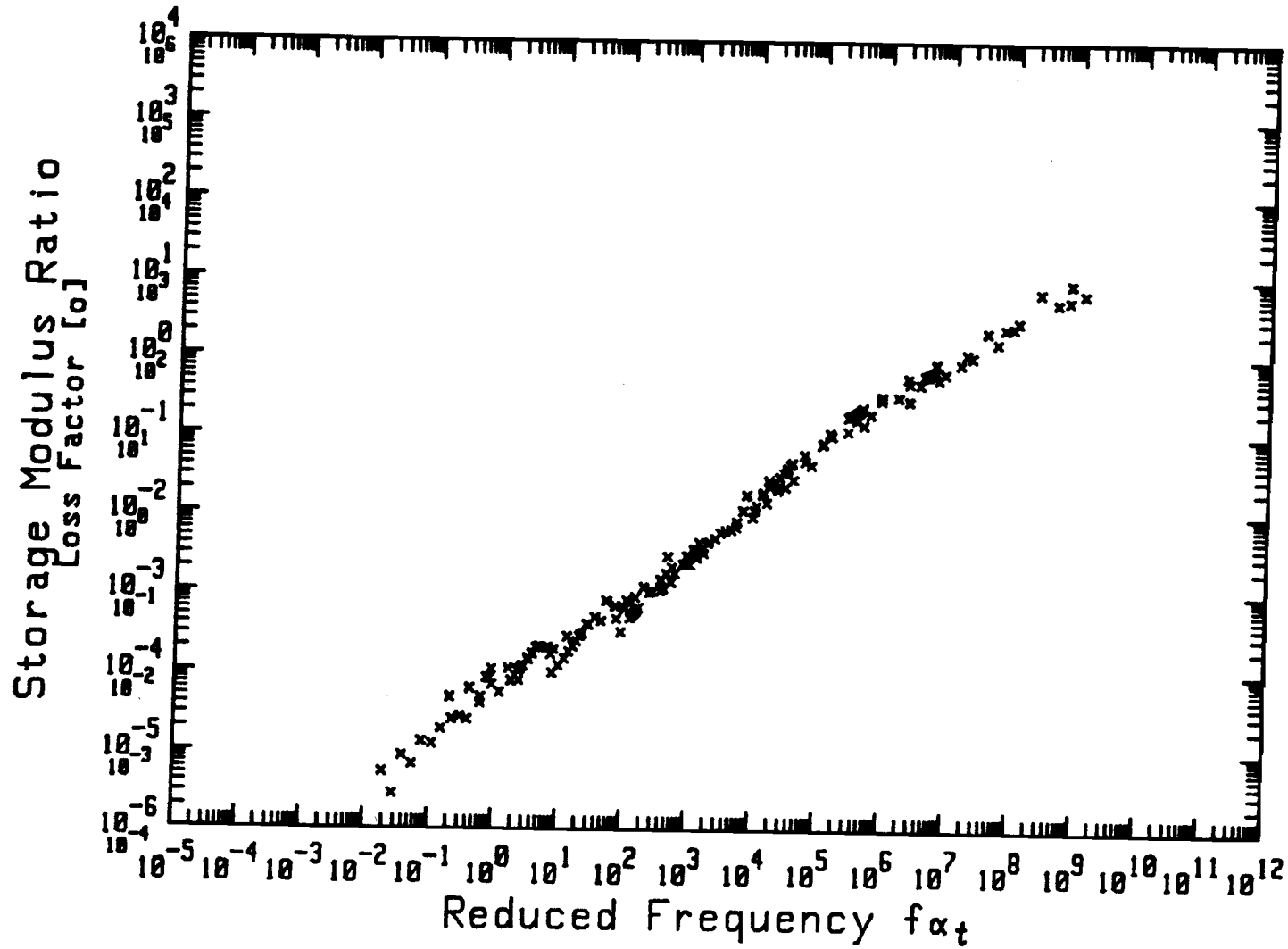


Figure 15: Plot of Modulus Ratio (G_e) Versus Reduced Frequency ($T_A = 8900^\circ R$)

FAC-27

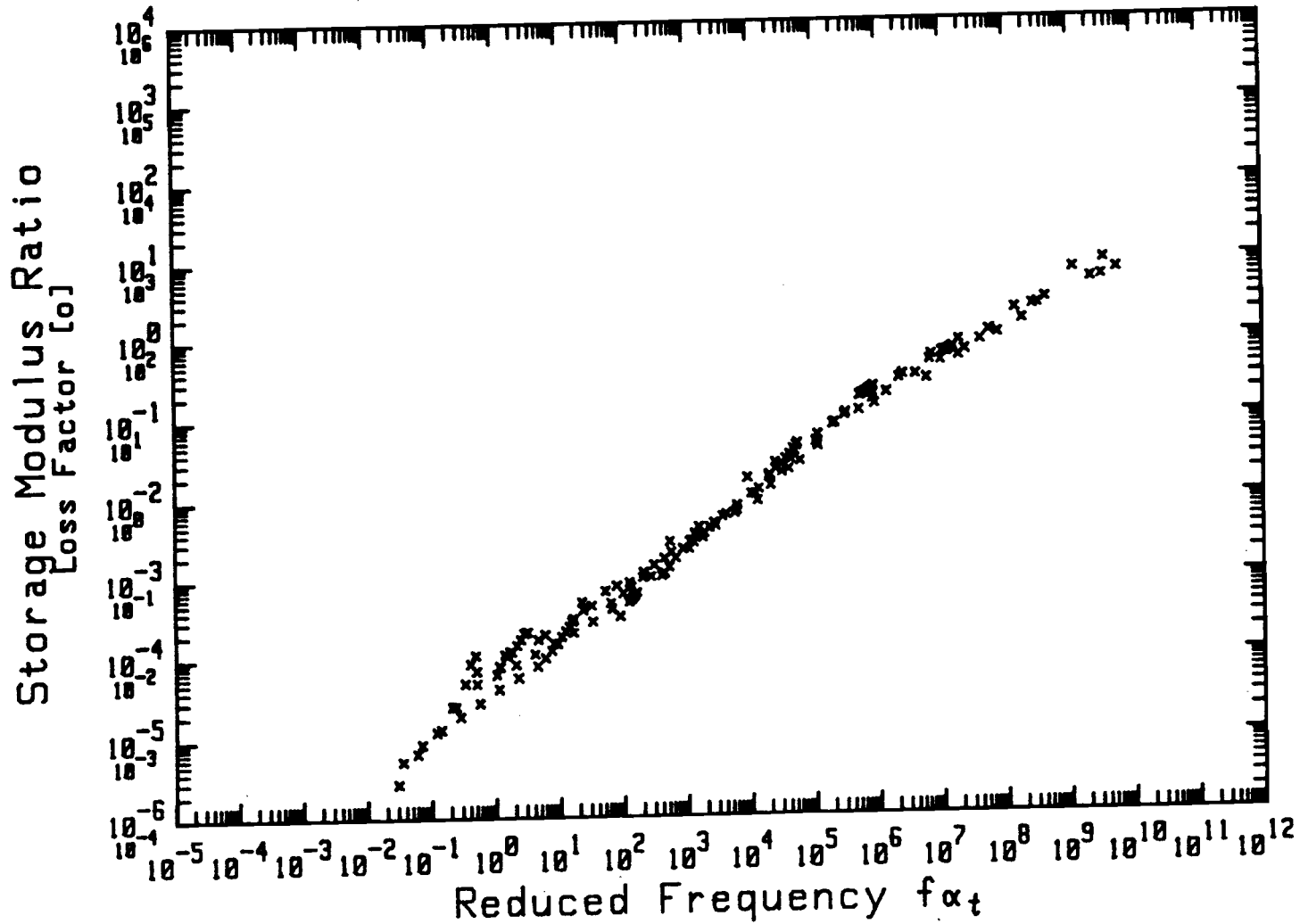


Figure 16: Plot of Modulus Ratio (G_e) Versus Reduced Frequency
 ($T_A = 10000^\circ R$)

FAC-28

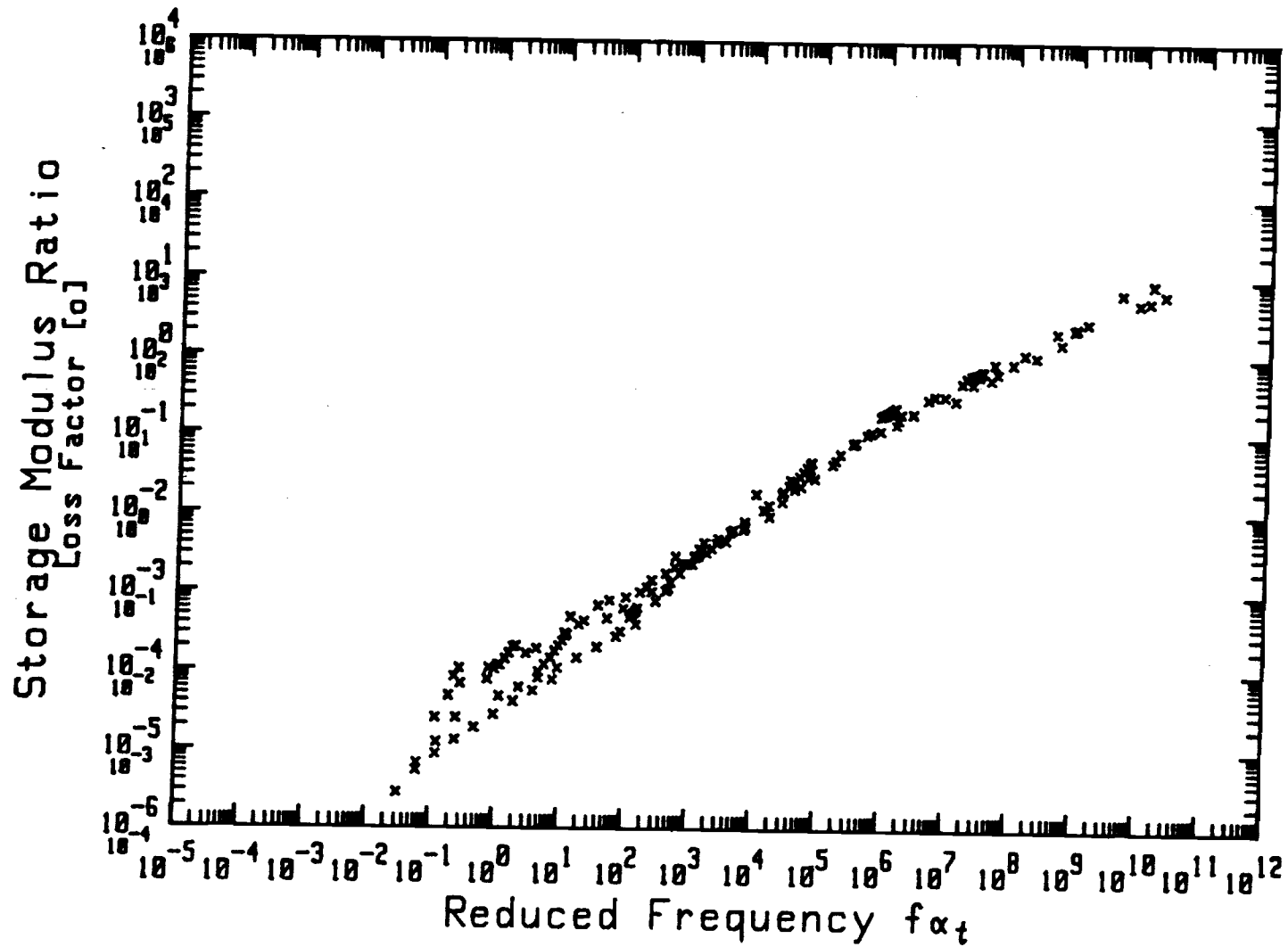


Figure 17: Plot of Modulus Ratio (G_e) Versus Reduced Frequency ($T_A = 11000^\circ R$)

FAC-29

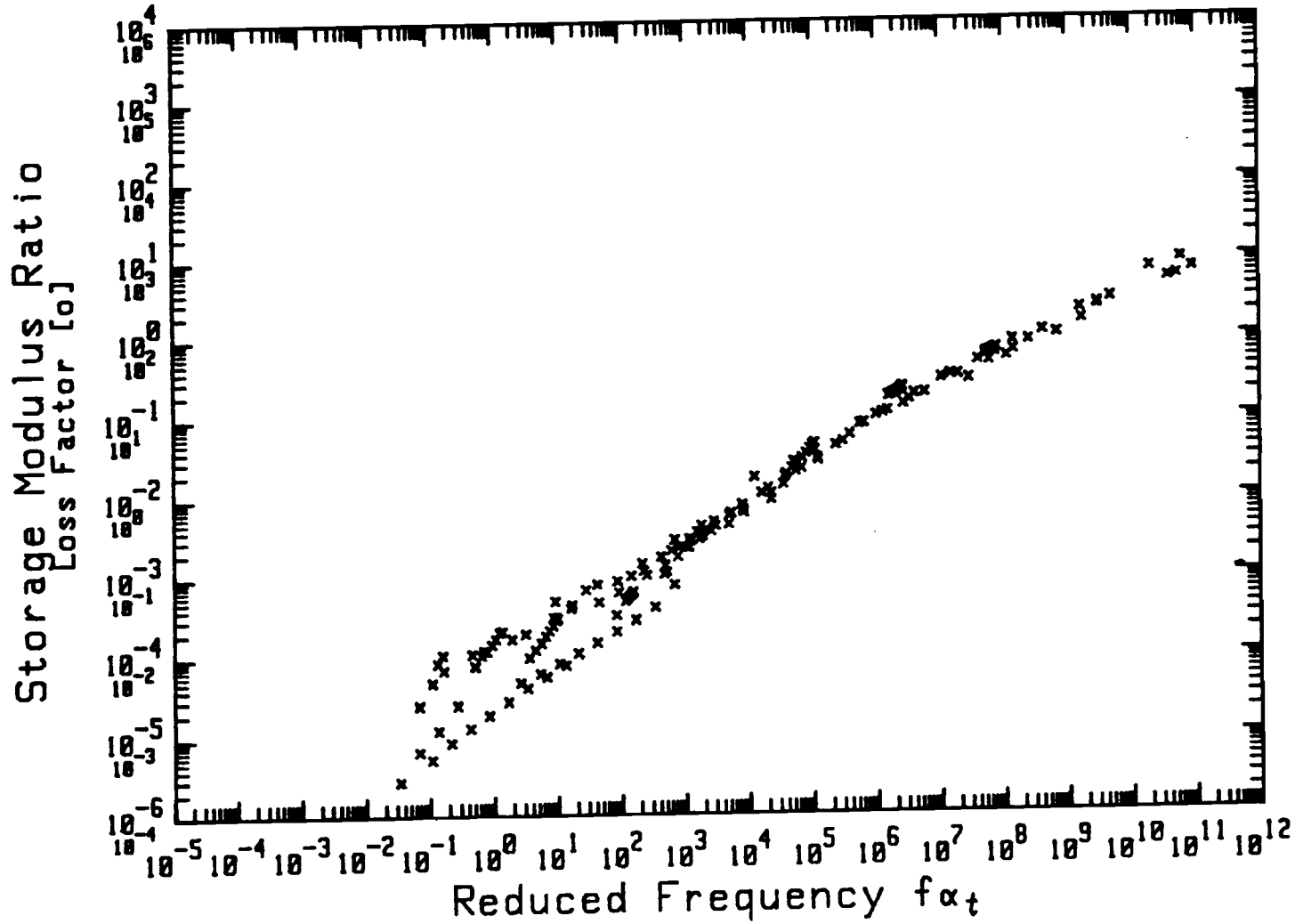


Figure 18: Plot of Modulus Ratio (G_e) Versus Reduced Frequency
 ($T_A = 12000^\circ R$)

FAC-30

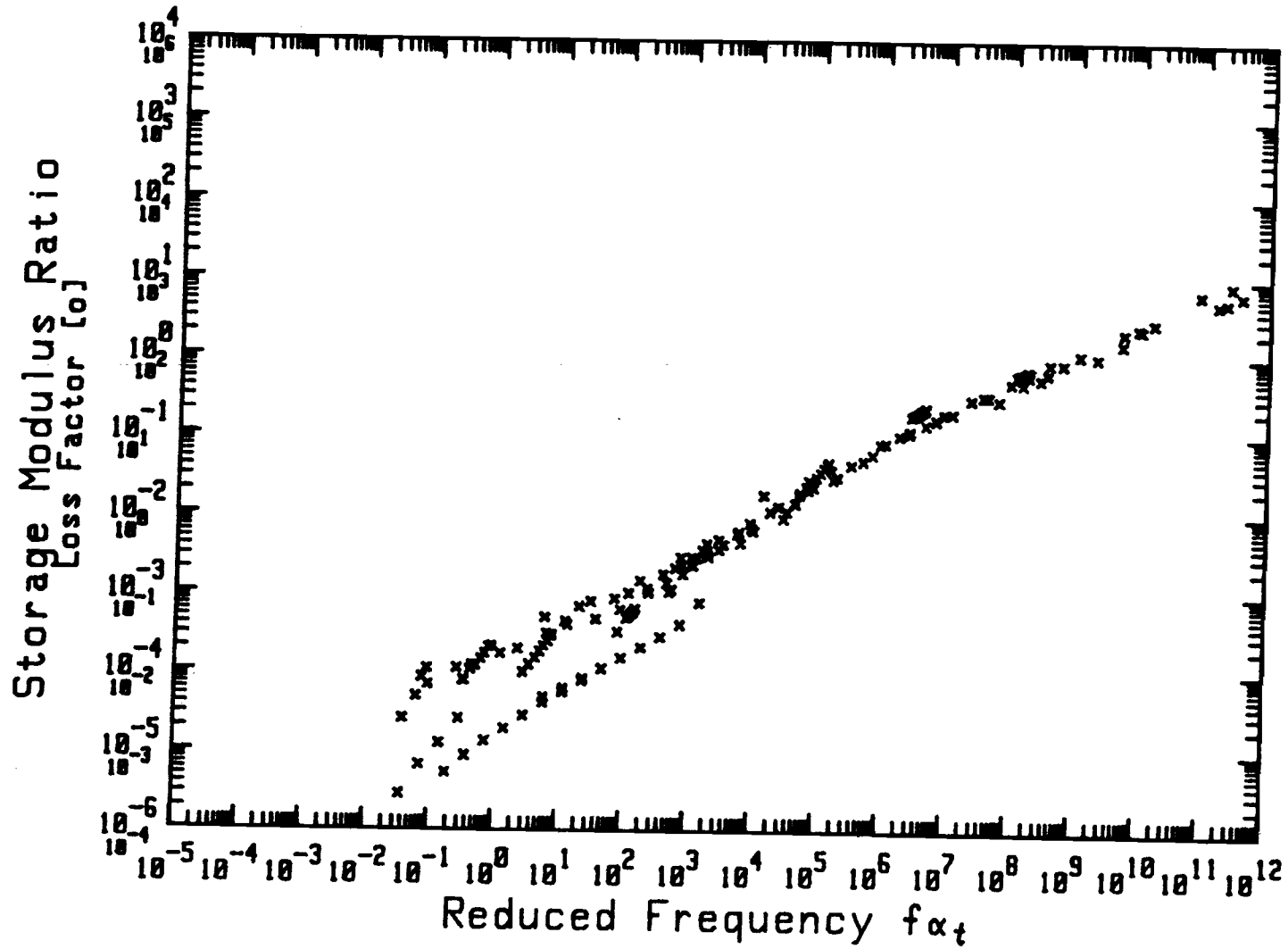


Figure 19: Plot of Modulus Ratio (G_e) Versus Reduced Frequency ($T_A = 13000^\circ R$)

FAC-31

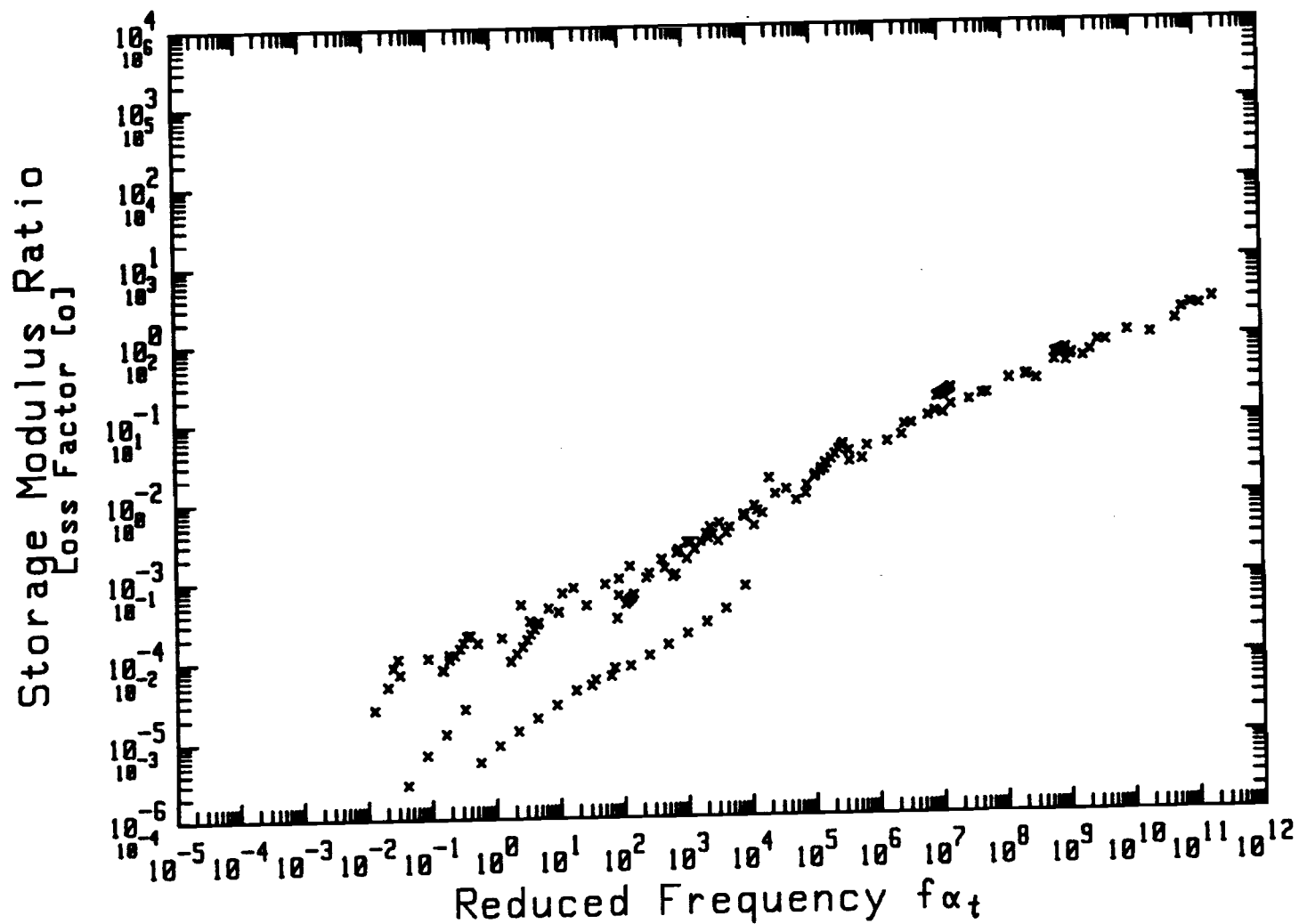


Figure 20: Plot of Modulus Ratio (G_e) Versus Reduced Frequency ($T_A = 15000^\circ R$)

FAC-32

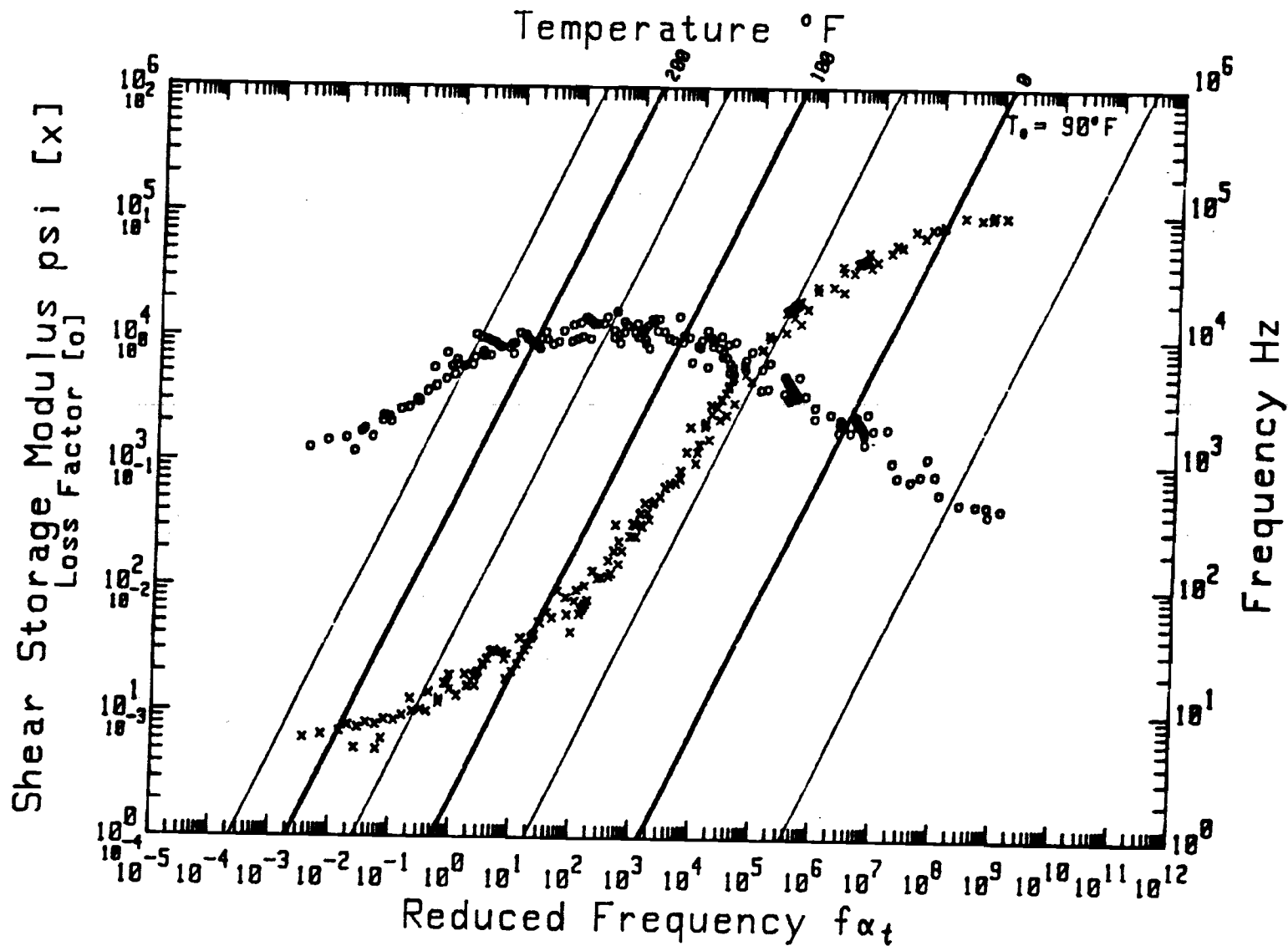


Figure 21: Reduced Frequency Nomogram for 3M Y-966 Adhesive
($T_A = 8900^\circ\text{R}$)